2013

Myxomavirus-derived serpin prolongs survival and reduces inflammation and hemorrhage in an unrelated lethal mouse viral infection

Herbert W. Virgin
Washington University School of Medicine in St. Louis
et al

Antimicrobial Agents and Chemotherapy

Myxomavirus-Derived Serpin Prolongs Survival and Reduces Inflammation and Hemorrhage in an Unrelated Lethal Mouse Viral Infection

Hao Chen, Donghang Zheng, Jeff Abbott, Liying Liu, Mee Y. Bartee, Maureen Long, Jennifer Davids, Jennifer Williams, Heinz Feldmann, James Strong, Katrina R. Grau, Scott Tibbetts, Colin Macaulay, Grant McFadden, Robert Thoburn, David A. Lomas, Francis G. Spinale, Herbert W. Virgin and Alexandra Lucas

Antimicrob. Agents Chemother. **2013, 57(9):4114. DOI: 10.1128/AAC.02594-12.**
Published Ahead of Print 17 June 2013.

AAC Journals.ASM.org

Myxomavirus-Derived Serpin Prolongs Survival and Reduces Inflammation and Hemorrhage in an Unrelated Lethal Mouse Viral Infection

Hao Chen,[a,b] Donghang Zheng,[a,b] Jeff Abbott,[c] Liying Liu,[a] Mee Y. Bartee,[a,b] Maureen Long,[c] Jennifer Davids,[a,b] Jennifer Williams,[a] Heinz Feldmann,[d]* James Strong,[d] Katrina R. Grau,[b] Scott Tibbetts,[b] Colin Macaulay,[e] Grant McFadden,[b,e] Robert Thoburn,[a] David A. Lomas,[f] Francis G. Spinale,[g] Herbert W. Virgin,[h] Alexandra Lucas[a,b,e]

Divisions of Cardiology and Rheumatology, Department of Medicine,[a] Department of Molecular Genetics and Microbiology,[b] and College of Veterinary Medicine,[c] University of Florida, Gainesville, Florida, USA; National Microbiology Laboratory, Public Health Agency of Canada, Winnipeg, Manitoba, Canada[d]; Viron Therapeutics, Inc., London, Ontario, Canada[e]; Division of Pulmonary Medicine, Department of Medicine, University of Cambridge, Cambridge, United Kingdom[f]; Department of Surgery, Medical University of South Carolina, Department of Cell Biology and Anatomy, South Carolina, USA[g]; Departments of Pathology and Immunology and Molecular Microbiology, Washington University, St Louis, Missouri, USA[h]

Lethal viral infections produce widespread inflammation with vascular leak, clotting, and bleeding (disseminated intravascular coagulation [DIC]), organ failure, and high mortality. Serine proteases in clot-forming (thrombotic) and clot-dissolving (thrombolytic) cascades are activated by an inflammatory cytokine storm and also can induce systemic inflammation with loss of normal *ser*ine *p*rotease *in*hibitor (serpin) regulation. Myxomavirus secretes a potent anti-inflammatory serpin, Serp-1, that inhibits clotting factor X (fX) and thrombolytic tissue- and urokinase-type plasminogen activators (tPA and uPA) with anti-inflammatory activity in multiple animal models. Purified serpin significantly improved survival in a murine gammaherpesvirus 68 (MHV68) infection in gamma interferon receptor (IFN-γR) knockout mice, a model for lethal inflammatory vasculitis. Treatment of MHV68-infected mice with neuroserpin, a mammalian serpin that inhibits only tPA and uPA, was ineffective. Serp-1 reduced virus load, lung hemorrhage, and aortic, lung, and colon inflammation in MHV68-infected mice and also reduced virus load. Neuroserpin suppressed a wide range of immune spleen cell responses after MHV68 infection, while Serp-1 selectively increased $CD11c^+$ splenocytes (macrophage and dendritic cells) and reduced $CD11b^+$ tissue macrophages. Serp-1 altered gene expression for coagulation and inflammatory responses, whereas neuroserpin did not. Serp-1 treatment was assessed in a second viral infection, mouse-adapted Zaire ebolavirus in wild-type BALB/c mice, with improved survival and reduced tissue necrosis. In summary, treatment with this unique myxomavirus-derived serpin suppresses systemic serine protease and innate immune responses caused by unrelated lethal viral infections (both RNA and DNA viruses), providing a potential new therapeutic approach for treatment of lethal viral sepsis.

In severe viral infections and sepsis, as for bacterial sepsis, there is high associated mortality, up to 40 to 70%, in viral infections where treatment is very limited (1–8). Once a patient is in shock, treatment options are often restricted to hemodynamic support. In septic states, widespread intravascular clotting and hemorrhage called disseminated intravascular coagulation (DIC) can occur, leading to microvascular thrombosis, organ damage, and shock (1–8). The excessive clot formation depletes coagulation factors, which, in turn, can cause excess bleeding (consumptive coagulopathy). Activation of thrombotic and thrombolytic proteases and also inflammatory responses is reciprocal (1–9). With dysregulated coagulation, there is massive upregulation of cytokines and other inflammatory mediators. This cytokine storm contributes to tissue damage, producing leaky capillaries (permeable blood vessels) and increasing virulence with, in some cases, dysfunctional immune responses (1–3).

Treatments for lethal sepsis and associated DIC that target thrombotic and thrombolytic pathways have been reported and include clot inhibitors, such as anti-thrombin III (9), activated protein C (10), tissue factor pathway inhibitor (TFPI), and thrombomodulin, as well as agents that block hemorrhage, such as factor VII (fVIII) (11). These approaches have produced only moderate (6 to 19%) reductions in death rates (5–11). Anti-inflammatory approaches, such as interleukin 10 (IL-10), for treatment of sepsis have also been tested, again with variable success in clinical trials (1–8). Additionally, low levels of protease activation, as in cancer and infection, can influence innate immune responses without overt coagulopathic or hemorrhagic changes. A combined therapeutic approach targeting both thrombotic and thrombolytic pathways, as well as associated excess inflammation, may be necessary to improve outcomes in severe septic states.

Large DNA viruses provide a new source of multifunctional immunomodulating proteins used as defenses that protect the virus against host attacks (12–14). Many such viral immuno-

Received 17 January 2013 Returned for modification 21 February 2013
Accepted 30 May 2013
Published ahead of print 17 June 2013

Address correspondence to Alexandra Lucas, alexandra.lucas@medicine.ufl.edu.
* Present address: Heinz Feldmann, Laboratory of Virology, Division of Intramural Research (DIR), National Institute of Allergy and Infectious Diseases (NIAID), National Institutes of Health (NIH), Rocky Mountain Laboratories, Hamilton, Montana, USA.

Supplemental material for this article may be found at http://dx.doi.org/10.1128/AAC.02594-12.

doi:10.1128/AAC.02594-12

modulators have evolved over millions of years to become highly potent and often point to central pathways that represent pivotal regulatory points in the immune response system and thus excellent targets for new therapeutic approaches. Myxomavirus secretes a serpin, Serp-1, that inhibits both thrombolytic and thrombotic proteases, as well as displaying marked anti-inflammatory activity in a wide range of animal models. Serp-1 inhibits tissue- and urokinase-type plasminogen activators (tPA and uPA) and plasmin in the clot-dissolving (thrombolytic) cascade and also factor X (fX) (13–15) in the clot-forming (thrombotic) cascade. Serp-1 also inhibits thrombin (factor II [fII]) in the presence of heparin, a glycosaminoglycan, but is cleaved by thrombin in the absence of heparin (15). Purified Serp-1 protein has proven anti-inflammatory activity in animal models of vascular injury after balloon angioplasty and stent implantation (12, 14, 16–18) and transplantation (18–21) and also in arthritis (22). In contrast, the mammalian serpin, neuroserpin (NSP), inhibits only tPA and uPA and not fII or fX (23), but it can reduce plaque growth and stroke volume in arterial injury models (21). Serp-1 has been successfully tested in a recent phase IIa trial for treatment of acute coronary syndromes with stent implant (24), with a statistically significant drop in two biomarkers of cardiovascular damage, indicating reduced ischemic injury that is in part caused by microembolization (24, 25). Serp-1 also produced a trend toward reduced D-dimer, a marker for dysfunctional coagulation (DIC) (14).

We examined the capacity of Serp-1 to improve outcome in two mouse models of lethal viral sepsis: gammaherpesvirus 68 (MHV68) infection in gamma interferon receptor (IFN-γR) knockout mice (26, 27) and mouse-adapted Zaire ebolavirus infections in BALB/c wild-type mice. MHV68 serves as a recognized model for human inflammatory vasculitis and lethal herpesvirus infections. To assess for the capacity to alter the course of a second unrelated hemorrhagic lethal virus infection in wild-type mice, Serp-1 treatment of mouse-adapted Zaire ebolavirus, a category A virus (28, 29), in BALB/c mice was also examined. MHV causes high mortality in IFN-γR knockout mice but not in wild-type mice. Ebolavirus is a filovirus that induces the bleeding diathesis seen in viral hemorrhagic fevers (VHF) and disables the immune response. Both infections result in more than 80% mortality in the mouse models, although the mouse-adapted Zaire ebolavirus does not induce the pulmonary hemorrhage seen in humans, while the MHV68-infected model does display severe pulmonary hemorrhage. Serp-1 and mammalian serpin, NSP, treatment were compared in MHV68-infected mice to differentiate effects of inhibition of thrombotic and thrombolytic proteases in infected mice.

MATERIALS AND METHODS

Ethics statement. All animal studies conform to local and national guidelines for animal care and experimentation. All procedures were approved by the University of Florida IACUC and by the Canadian Science Centre for Human and Animal Health (CSCHAH) Animal Care Committee, NML, PHAC (Winnipeg, Manitoba, Canada).

MHV68 passage and preparation. MHV68 was provided by the laboratory of H. Virgin (26, 27). Viral MHV68 stocks were generated in 3T12 cells (ATCC, Manassas, VA). 3T12 cells were cultured in medium consisting of Dulbecco modified Eagle medium (DMEM), 10% fetal calf serum (FCS), 10 mM HEPES, 2 mM L-glutamine, and 1% penicillin or streptomycin. At 50% confluence, cells were infected at a multiplicity of infection (MOI) of 0.1. Seven days postinfection, cells underwent freeze-thaw and the lysate was transferred to Nalgene Oak Ridge polypropylene copolymer (PPCO) tubes and centrifuged (15 min at 4,300 × *g*). Cleared supernatant was centrifuged for 2 h at 12,000 × *g*. The pellet was rinsed with phosphate-buffered saline (PBS), resuspended in medium, vortexed, and stored at −80°C in 250-μl aliquots. Virus titers were determined in duplicate.

Ebolavirus source. The 1976 Mayinga isolate of ebolavirus from Zaire (now the Democratic Republic of the Congo) (4, 28, 29) was isolated from a human specimen on Vero E6 cells and passaged twice prior to initiation of these experiments. Focus-forming units (FFU) for Zaire ebolavirus were assayed by Ebola virus matrix protein (VP40)-specific antiserum.

Protein expression and purification. Serp-1 protein was kindly provided by Viron Therapeutics Inc. (London, Ontario, Canada). Serp-1 was purified from supernatant of recombinant Chinese hamster ovary (CHO) cells by sequential column chromatographic separation as described previously (14–20, 23). Serp-1 protein was 354 amino acids, with a purity greater than 99% monomer as determined by overloaded colloidal blue gels (see Fig. S1 in the supplemental material) and reverse-phase high-performance liquid chromatography (HPLC). Purified Serp-1 protein has 94.5% potency for uPA inhibition activity assayed by chromogenic assay as previously described.

NSP protein was expressed in BL21(DE3) pLysS cells (Invitrogen, Carlsbad, CA) (21). Medium containing LB, ampicillin (Amp), and chloramphenicol (Cap) was inoculated with cells and grown to an optical density (OD) of 0.5 at 600 nm and 37°C at 250 rpm. Cells were cooled to 16°C and induced with 1 mM IPTG (isopropyl β-D-1-thiogalactopyranoside) and pelleted. Cell pellets were resuspended in lysis buffer (20 mM Tris, 20 mM imidazole, 150 mM NaCl) containing EDTA-free complete protease inhibitors (Roche) and 2 mM 4-(2-aminoethyl) benzenesulfonyl fluoride hydrochloride (AEBSF). Samples were French pressed, and the cell debris was pelleted at 15,000 rpm. Supernatant was loaded onto equilibrated cobalt-nitrilotriacetic acid (NTA) (Sigma-Aldrich, St. Louis, MO), washed with 100 volumes of lysis buffer, and eluted with elution buffer (20 mM Tris, 150 mM imidazole, 150 mM NaCl). NSP was dialyzed into 0.9% saline and concentrated using a 10-kDa-cutoff Amicon Ultra (Millipore) and then passed through a 0.22-μm filter (Millipore). A single band was also detected for NSP by gel electrophoresis and inhibitory activity measured for uPA or tPA by chromogenic assay (data not shown; Assaypro, St. Louis, MO) (14, 15, 17–21, 24).

Experimental animal protocols. Pure IFN-γR knockout (IFN-γR$^{-/-}$) mice (B6.129S7-*Ifngr1*^{tm1Agt}/J) and wild-type mice (BALB/c), 5 to 7 weeks of age, were purchased from JaxLabs (Sacramento, CA) and bred under specific-pathogen-free conditions. Littermate controls were used for all studies.

MHV68 infection. Ninety (6 to 10 mice per group) IFN-γR$^{-/-}$ mice were infected by intraperitoneal (i.p.) injection of 12.5 × 10^6 PFU or 6 × 10^6 PFU of MHV68 given in 0.1 ml of DMEM (26). Mice were treated with either saline control (100 μl), Serp-1 (100 μg/kg of body weight/100 μl) or NSP (100 μg/kg/100 μl) given at the time of infection and then daily by i.p. injection for a total of 10 days starting on the day of MHV68 infection. Serp-1 treatment was also tested with 10 days of treatment starting 21 days postinfection ($n = 12$) or with 30 days of treatment starting on the day of infection ($n = 10$) or starting 7 days postinfection ($n = 12$). Mice were monitored up for 10 days and 5, 12, and 15 weeks. Mice were carefully monitored by the veterinary animal care staff to minimize potential suffering. Euthanasia was performed as previously described (14–21).

***In vitro* MHV68 replication assay.** NIH 3T12 murine fibroblasts were infected *in vitro* with wild-type MHV68 at an MOI of 0.05 in the absence or presence of 500 ng/ml of Serp-1. At 96 h postinfection, cells and supernatant fluid were harvested, and viral titers were determined by plaque assay. Plaque assays were performed on NIH 3T12 cells. Briefly, 10-fold serial dilutions of samples were prepared in serum-free DMEM, and then infections were performed in 400 μl at 37°C for 1 h. Cells were then overlaid with a 1:1 mixture of methylcellulose (Sigma) and MEM supplemented with 10% fetal calf serum and antibiotics. At 7 days postinfection, plaques were visualized by neutral red staining and counted.

Ebolavirus infection. Wild type BALB/c mice were infected i.p. with a mouse-adapted Zaire ebolavirus 1976 Mayinga strain (10× the 60% lethal dose [LD_{60}]). Immediately prior to infection, mice were treated with either saline or Serp-1 at 5-, 50-, or 100-μg/kg doses given by intravenous (i.v.) tail vein bolus. Subsequent daily i.p. injections of control saline or Serp-1 were given for a total of 10 daily doses or until euthanasia. The usual survival time is 6 to 7 days after ebolavirus infection, and based upon this, treated mice that survived past this point were monitored for a total of 14 days and then euthanized whether ill or healthy. Mice were maintained in the biosafety level 4 (BSL4) facility in Winnipeg, Manitoba, Canada (J. Strong and H. Feldmann). Tissues were harvested and frozen for histopathological analysis. In a second series of mouse infections, mice were euthanized at 6 days after ebolavirus infection and tissues taken for pathological and quantitative reverse transcription-PCR (qRT-PCR) genome analysis (FFU equivalent) examination as follows. RNA was isolated from these tissue samples by homogenization in 0.25% trypsin-EDTA with subsequent extraction using a QIAampViralRNA minikit (Qiagen). ZEBOV-GP (Zaire ebolavirus glycoprotein) was detected using the LightCycler 480 RNA Master hydrolysis probe (Roche Diagnostics) and the following: forward primer, 5′-GGCCAACGAGACGACTCAA-3′; reverse primer, 5′-AAAGGTGCGTAGCTCAGTTGTG-3′; and probe, 6-carboxyfluorescein (FAM)-CTCTTCAACTGTTCCTGAGAG-MGBNFQ. All samples were run on a Smart Cycler (ABI Biosystems) through quantitative RT-PCR. All samples were quantified by being run against known serially diluted samples extracted and run as described above. The limit of sensitivity of the ZEBOV GP-specific quantitative RT-PCR is ~0.1 FFU/ml.

Histological and morphometric analysis. At follow up, mice were euthanized and organ tissue harvested as well as blood samples. All specimens from MHV68-infected mice, with or without serpin treatment, were cut into 2 equal lengths (aorta, 3 to 5 mm, and other organs, 0.5 cm) and then cut into halves, one for histology and one for mRNA and protein analysis. Sections from ebolavirus-infected mouse tissues were fixed in BSL4 facility following approved standard operating protocols and then used for histology. For histology, sections were fixed in neutral buffered formalin (NBF), embedded in paraffin, and cut into 4-μm-thick cross sections and stained with hematoxylin and eosin (H&E), as described previously (14–21). Cellular invasion and tissue hemorrhage and necrosis were measured using an Olympus DP71 camera attached to an BX51 microscope (Olympus America Inc., Center Valley, PA) and quantified using Image Pro 6.0 (MediaCybernetics Inc., Bethesda, MD) (14–21).

Cytokine assays. Blood samples (1 ml) were obtained from MHV68-infected mice at the time of sacrifice, placed in chilled EDTA tubes, and centrifuged, and plasma was stored at −80°C. At the time of assay, plasma samples were subjected to multiplex array for cytokines (human MAP base kit LUH000; R&D Systems, Minneapolis, MN) and measured simultaneously, minimizing interassay variability. Multiplex array was validated using internal controls for each cytokine (30). Levels of IL-1β, IL-2, IL-4, IL-6, tumor necrosis factor alpha (TNF-α), IFN-γ, and granulocyte-macrophage colony-stimulating factor (GM-CSF) in plasma were measured. Plasma samples (20 μl) were undiluted. The relative fluorescence for each cytokine (Bio-Plex 200; Bio-Rad Laboratories, Hercules, CA) was converted to an absolute concentration using calibration curves generated from known recombinant standards. The average sensitivity for cytokines was 0.3 pg/ml. The coefficient of variation for these assays was 15% or less. IL-10 was additionally measured in plasma samples using an enzyme-linked immunosorbent assay (ELISA) kit (31–33).

IHC. Immunohistochemical (IHC) staining of invading cells was performed using a rabbit-specific horseradish peroxidase (HRP)/diaminobenzidine (DAB) detection IHC kit (ab64261; Abcam, Cambridge, MA) per the manufacturer's protocol (14–21). Tissue sections were stained as previously described with primary antibodies (anti-MHV68 polyclonal rabbit serum and preimmune rabbit serum provided by H. Virgin [26, 27], 1:500 for MHV68 detection, 1:100 for $CD3^+$ T cells, and 1:400 for $CD11b^+$ macrophages) with secondary rabbit-specific HRP-conjugated antibody for MHV68, CD3, and CD11b staining. Sections were counterstained with hematoxylin. Positively stained cells were counted in three high-power-field (HPF) areas in each tissue section. No staining was observed in infected tissues incubated with preimmune serum or in uninfected tissues incubated with immune serum.

Flow cytometry. Splenocytes isolated from one mouse were not present in high enough counts for flow cytometry analysis; therefore, spleen cells from the same experimental group were pooled and stained with antibodies to surface or intracellular antigens and incubated for 30 min at room temperature (21). Labeled cells were washed and resuspended with 150 μl of PBS and assessed by flow cytometry. For staining of intracellular antigens, cell pellets in 500 μl were incubated with fixation-permeabilization buffer (eBioscience, San Diego, CA), incubated in the dark for 45 min, treated with permeabilization buffer (eBioscience), and incubated with intracellular antibody mix, with further incubation for 30 min at 4°C. All antibodies were purchased from eBiosciences and Biolegend (San Diego, CA) (see Table S4 in the supplemental material). Table S1 in the supplemental material lists immune cell types analyzed and corresponding fluorochrome-labeled antibodies. Flow cytometry was performed with a CyAn ADP Analyzer (Dako, Fort Collins, CO) (14, 21, 32). Data were analyzed using Gatelogic software (eBioscience).

RT-PCR analysis of aortic specimens. MHV68-infected mouse aortic sections were collected in RNA Later (Ambion, Austin, TX), and RNA was isolated using an RNeasy minikit by following the manufacturer's protocol (Qiagen, Valencia, CA). RNA was reverse transcribed to cDNA using a Superscript VILO cDNA synthesis kit (no. 11754-250; Invitrogen Corporation, CA), and real-time PCR was carried out using a SYBR green core reagent kit and a model 7300 RT-PCR system (Applied Biosystems, Austin, TX) (14, 20, 21, 32). Primers are listed in Table S2 in the supplemental material.

Bleeding time assays. For the bleeding assay, mice were anesthetized with ketamine and xylazine (80 mg/kg and 5 mg/kg), the tail was prewarmed for 5 min in 10 ml of saline at 37°C in a water bath, and a 3-mm tail segment was amputated and immediately returned to the saline. Bleeding time was measured as the time between the start of bleeding to cessation of bleeding.

Statistical analysis. Statistical analysis was performed using Statview, version 5.01 (SAS, Inc., Cary, NC) (14–21). Survival was assessed by Kaplan-Meier analysis. Only mice requiring early euthanasia prior to the designated follow-up time were included in survival analyses. Mean cell counts or areas of tissue hemorrhage or necrosis were calculated from three sections for each specimen isolated from each mouse. Mean values were used for subsequent statistical analyses. Multiple-group comparisons were performed using analysis of variance (ANOVA) with Fisher's protected least significant difference (PLSD) and unpaired two-tailed Student's *t* test for subgroup analysis (12–21, 23). A P value of ≤ 0.05 is considered significant.

RESULTS

Serp-1 prolongs survival in herpesvirus (MHV68)-infected mice. In an initial study, Serp-1 treatment was given by daily intraperitoneal (100 μg/kg) injections for the first 10 days postinfection (6×10^6 to 12.5×10^6 PFU) starting on the day of MHV68 infection. With 10 days of treatment, Serp-1 significantly prolonged survival in gamma interferon receptor-deficient mice (B6.129S7-*Ifngr1*^{tm1Agt}/J, IFN-γ$R^{-/-}$) ($P \leq 0.048$; Fig. 1A). Saline-treated MHV68-infected mice survived for up to 42 days, whereas Serp-1-treated mice survived for up to 55 days ($n = 60$ mice, 6 to 12 mice/group) (Table 1). Early improved survival with Serp-1 treatment was lost by 12 weeks postinfection. NSP treatment (100 μg/kg i.p. for 10 days) (Table 1) in a separate series of MHV68-infected IFN-γ$R^{-/-}$ mice did not improve survival, with a trend toward increased mortality (Fig. 1B) ($P = 0.079$; $n = 16$).

In a subsequent study, prolonged daily treatment with Serp-1

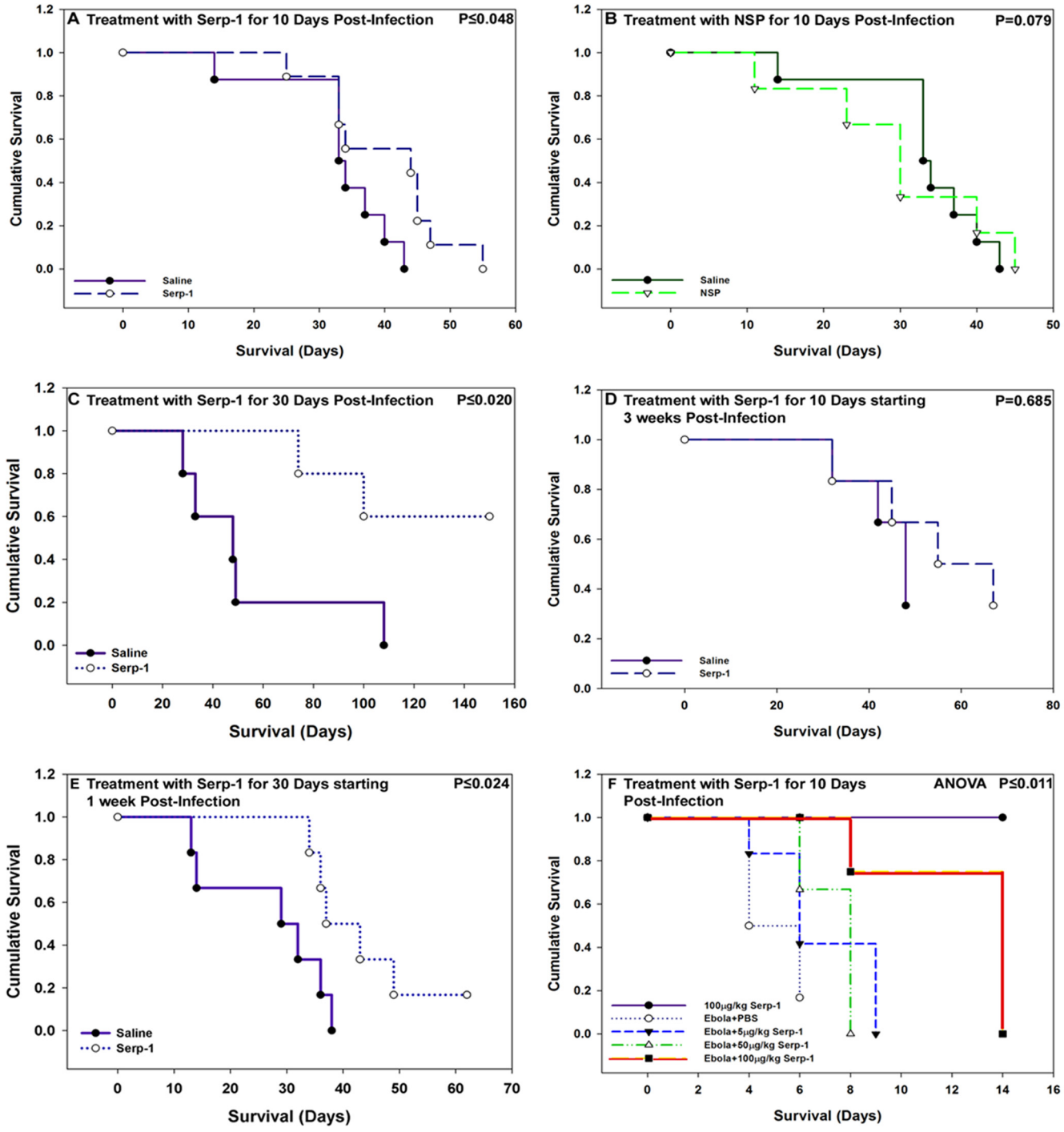

FIG 1 Serp-1 prolongs survival in MHV68-infected IFN-$\gamma R^{-/-}$ mice and in wild-type ebolavirus-infected BALB/c mice. (A) Treatment with Serp-1 (100 μg/kg/day) for 10 days beginning immediately after MHV68 infection in IFN-$\gamma R^{-/-}$ mice prolonged early survival ($P \leq 0.048$) by approximately 10 days ($n = 60$ mice). (B) Treatment with NSP given immediately after MHV68 infection for 10 days did not improve survival, with a trend toward increased mortality compared to saline ($P = 0.079$; $n = 12$). (C) Treatment with Serp-1 for the first 30 days postinfection, beginning on the day of infection, further prolonged survival in MHV68-infected IFN-$\gamma R^{-/-}$ mice compared to the saline-treated mice ($P \leq 0.02$; $n = 10$). (D) Treatment for 10 days with Serp-1 beginning 21 days after MHV68 infection produced only a nonsignificant trend toward improved survival ($P = 0.326$; $n = 12$). (E) Treatment with Serp-1 for 30 days beginning 7 days postinfection again significantly improved survival ($P \leq 0.025$; $n = 12$). (F) Serp-1 treatment at 100 μg/kg/day similarly improved survival in ebolavirus-infected BALB/c mice but did not alter survival at lower doses (ANOVA, $P \leq 0.011$) (Kaplan-Meier survival analysis).

TABLE 1 Numbers of MHV68-infected IFNγR$^{-/-}$ mice and ebolavirus-infected BALB/c mice[a]

Mouse strain	Virus	Total no. of mice	No. treated with:					Treatment (days)		
			Saline, 100 μl	Serp-1			NSP, 100 μg	Start	Length	Follow-up
				5 μg	50 μg	100 μg				
IFN-γR$^{-/-}$	MHV68	14	7			7		0	10	10
	MHV68	23	12			23		0	10	35 (5 wks)
	MHV68	8	4			4		0	10	84 (12 wks)
	MHV68	16	8			8		0	10	105 (15 wks)
	MHV68	12	6			6		21	10	140 (20 wks)
	MHV68	10	5			5		0	30	140 (20 wks)
	MHV68	12	6			6		7	30	140 (20 wks)
	MHV68	14	7				7	0	10	10
	MHV68	16	8				8	0	10	56 (8 wks)
BALB/c	None		7					0	10	10
	Ebolavirus	6	6					0	10	14
	Ebolavirus	6		6				0	10	14
	Ebolavirus	6			6			0	10	14
	Ebolavirus	6				6		0	10	14

[a] Treatment start is the time when treatment was begun, day 0 is the day of viral infection, length of treatment is the duration of daily injections or treatments, and follow-up is the planned follow-up times postinfection. "μg" is used for "μg/kg."

starting on the day of infection and continuing for the first 30 days postinfection (100 μg/kg i.p.) prolonged survival even further in MHV68-infected IFN-γR$^{-/-}$ mice, for up to 150 days (Fig. 1C) ($P \leq 0.02$; $n = 10$). Of the 30-day-treated mice infected with MHV68, all mice treated with Serp-1 were alive for up to 80 days, and three of the five mice were alive for up to 150 days. In contrast, four out of the five saline-treated mice were dead by 50 days. Serp-1-treated mice with prolonged survival were euthanized at 150 days for a study analysis, although appearing healthy. Treatment with Serp-1 starting at 3 weeks after MHV68 infection produced a nonsignificant trend toward improved survival (Fig. 1D) ($P = 0.685$; $n = 12$). However, when Serp-1 treatment was begun at 1 week postinfection, there was again a significantly improved survival (Fig. 1E) ($P \leq 0.024$; $n = 12$), with survival for up to 150 days, at which time mice that remained healthy were euthanized. On general inspection, mice treated with Serp-1 for 10 days displayed fewer signs of infection, with reduced lethargy and hunching, and with 30 days of Serp-1 treatment, the MHV68-infected mice had ongoing freedom from signs of disease or sepsis.

Serp-1 reduced mortality in the ebolavirus mouse model. In a separate pilot study of ebolavirus infection performed in a BSL4 facility (HF, National Microbiology Laboratory, Public Health agency, Winnipeg, Manitoba, Canada), in 24 BALB/c mice (6 mice/treatment group), treatment with Serp-1 at 5 to 100 μg/kg reduced tissue inflammation, necrosis, and necessity for euthanasia after virus infection (10× the LD_{50} of mouse-adapted Zaire ebolavirus) (Fig. 1F) ($P \leq 0.011$; $n = 24$ mice) (see also Table S1 in the supplemental material). Survival was increased from 6 to an average of 10 to 14 days after treatment with Serp-1 at 100 μg/kg for 10 days (first dose i.v. prior to infection, followed by 9 days of i.p. dosing). Serp-1 treatment at the lower doses did not prolong survival or reduce tissue necrosis. The usual survival time is 6 to 7 days after ebolavirus infection, and based on predicted survival, mice were euthanized at 14 days, irrespective of signs of infection. There was 90 to 100% mortality rate in untreated animals.

Serp-1 treatment reduced detectable infecting virus. MHV68 was detected in infiltrating mononuclear cells in the aortic adventitia (Fig. 2A), lung epithelium (Fig. 2C), and colon (Fig. 2E) on immunostained tissue sections. Serp-1 treatment for 10 days beginning immediately after MHV68 infection reduced positive staining for MHV68 in the lungs (Fig. 2D) and colon (Fig. 2F) compared to that for saline-treated mice ($P \leq 0.004$ and 0.015, respectively) (Fig. 2G). Serp-1 produced a nonsignificant trend toward reduced aortic staining for MHV68 (Fig. 2B and G) ($P = 0.168$). RT-PCR analysis detected a nonsignificant (2.5- to 10-fold) reduction in the MHV68 genome after Serp-1 treatment compared to saline (for HV DNA binding protein, 2.5-fold reduction [$P = 0.740$]; for HV capsid, 10-fold reduction [$P = 0.250$]; see RT-PCR data analysis in Fig. 7A). *In vitro* analysis of Serp-1 treatment on MHV68 proliferation in NIH 3T12 cells did not detect a significant difference in viral titers (see Fig. S2 in the supplemental material). RT-PCR detected a similar reduction in FFU equivalents (ZEBOV GP) for ebolavirus-infected mice with Serp-1 treatment at 100-μg/kg doses (Fig. 2H) at 6 days postinfection, but not with lower doses. Only 1 or 2 of the ebolavirus-infected mice were tested for FFU; thus, standard error (SE) cannot be computed. The lower mortality rate in both lethal infections correlated well with reduced detected virus (Fig. 2G and H).

Serp-1, but not NSP, reduces pulmonary consolidation and hemorrhage and gastrointestinal dilation after MHV68 infection. MHV68-infected IFN-γR$^{-/-}$ mice were followed up at 10 days and at 5, 12, and 15 weeks. Sixteen out of 31 saline-treated mice (51.2%) had pulmonary consolidation and hemorrhage. Pulmonary hemorrhage and consolidation were significantly reduced by Serp-1 treatment, with only 3/29 mice displaying pulmonary pathology (10.3%; $P \leq 0.01$). The gastrointestinal (GI) tract (esophagus to colon) had marked dilatation in 6 saline-treated mice (19.3%), but there was no dilatation of the GI tract with Serp-1 treatment ($P \leq 0.02$) (data not shown). Pulmonary and GI inflammation were associated with early mortality (Pearson's $R = 0.739$ and 0.668, respectively).

At 10 days of follow-up, saline-treated IFN-γR$^{-/-}$ mice had marked aortic adventitial inflammatory cell invasion, with less aggressive invasion in the media (Fig. 3A). The lungs (Fig. 3C) and

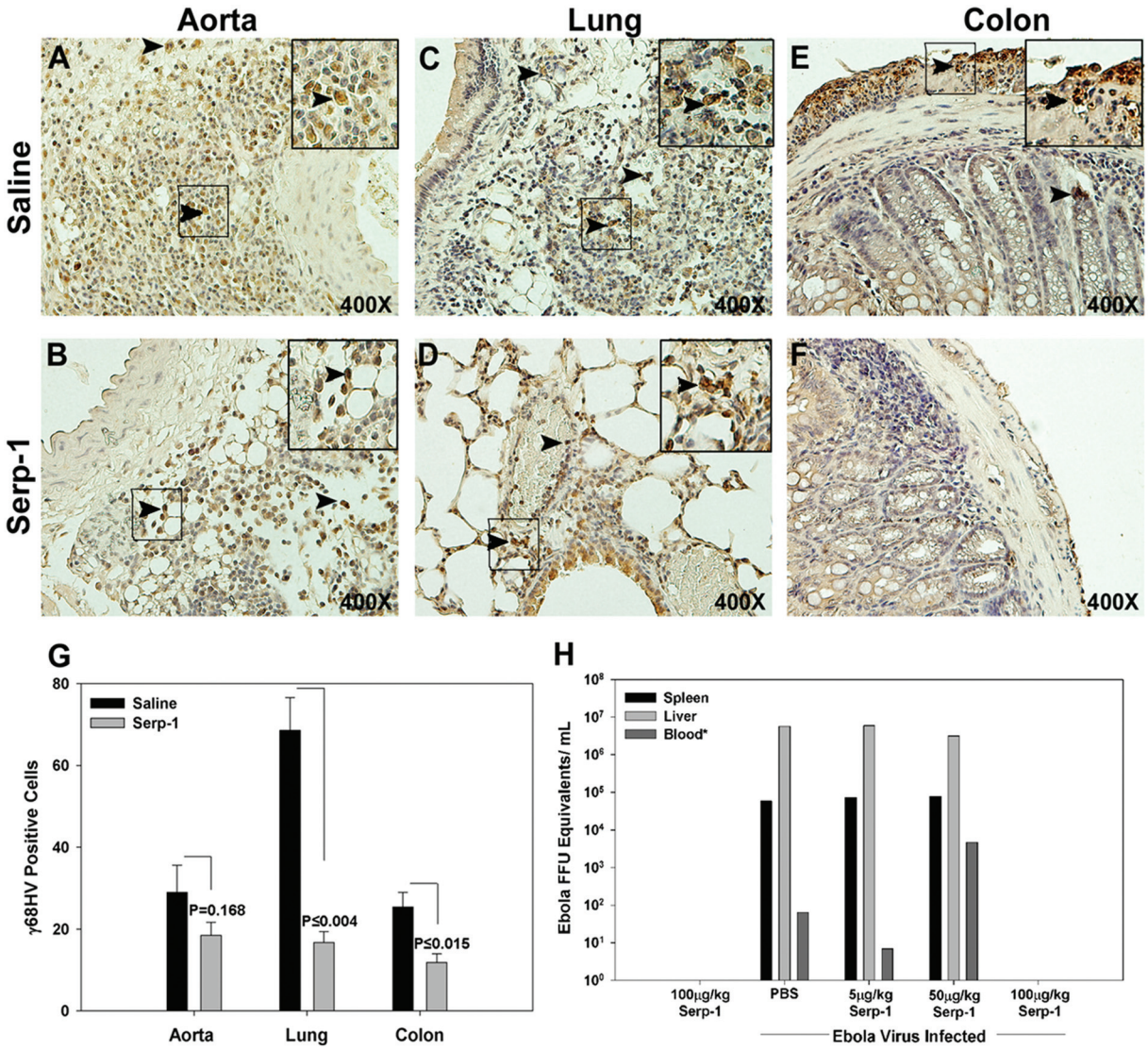

FIG 2 Serp-1 treatment reduces detectable MHV68 antigen expression in IFN-γR$^{-/-}$ mice at 10 days' follow-up and ZEBOV GP expression (FFU equivalents) for ebolavirus in BALB/c mice at 14 days' follow-up. Immunohistochemical staining for MHV68 at 10 days' follow-up demonstrated positively stained mononuclear cells (brown) in aortic (A), lung (C), and colon (E) histologic sections from saline-treated IFN-γR$^{-/-}$ mice. Positively stained cells were detected predominantly in the aortic adventitial layer (A), in interstitial and bronchial epithelial layers in the lung (C), and in submucosa and serosa in the colon (E). Positively stained cells (mean count per high-power field) were significantly reduced with Serp-1 treatment in lung (D and G) and colon (F and G) sections ($P \leq 0.004$ and $P \leq 0.015$, respectively; $n = 14$), with only borderline reductions in aorta (B and G). Arrowheads indicate cells staining positively for MHV68. FFU equivalents for ebolavirus were also reduced with Serp-1 treatment at 100-μg/kg doses for 10 days but not with lower Serp-1 doses at 6 days' follow-up (H) ($n = 31$). SE cannot be calculated for the ebolavirus FFU measurements, as only 2 representative mice were tested. For MHV68-positive IHC-stained sections, the magnification is ×400. Insets represent higher-power (×1,000) magnification.

colon (Fig. 3E) also had marked inflammatory mononuclear cell invasion. Serp-1 treatment significantly reduced inflammatory cell invasion in the aortic adventitia (Fig. 3B and J) ($P \leq 0.010$) and lungs (Fig. 3D and J) ($P \leq 0.047$) and demonstrated a trend toward reduced inflammatory cell invasion in the GI tract (Fig. 3F and J) ($P = 0.270$). At 5, 12, and 15 weeks, there was a less pronounced, ongoing trend toward reduced inflammation in aorta, lung, and colon sections (not shown).

NSP treatment increased inflammatory cell invasion in MHV68-infected mice compared to saline-treated mice. NSP-treated mice had significantly increased cell invasion into the aortic adventitia (Fig. 3G and K) ($P \leq 0.020$), the lung interstitium (Fig. 3H and K) ($P \leq 0.009$), and the colon submucosa (Fig. 3I and K) ($P \leq 0.018$) compared to saline (Fig. 3A and C, E, and K, respectively). There was, however, no GI dilatation seen in NSP-treated mice.

Early CD11b$^+$ macrophage invasion was significantly reduced with Serp-1 treatment after MHV68 infection. Serp-1 treatment for 10 days reduced CD11b-positive cell counts in aorta (Fig. 4A, D, and G) ($P \leq 0.048$) and lung (Fig. 4B, E, and G; $P \leq 0.005$) tissue sections from MHV68-infected mice at 10 days. No significant differences in macrophage counts were detected in colon with Serp-1 treatment (Fig. 4C, F, and G) ($P = 0.096$). In contrast, Serp-1 did not alter CD3$^+$ T cell counts in aorta (Fig. 4H,

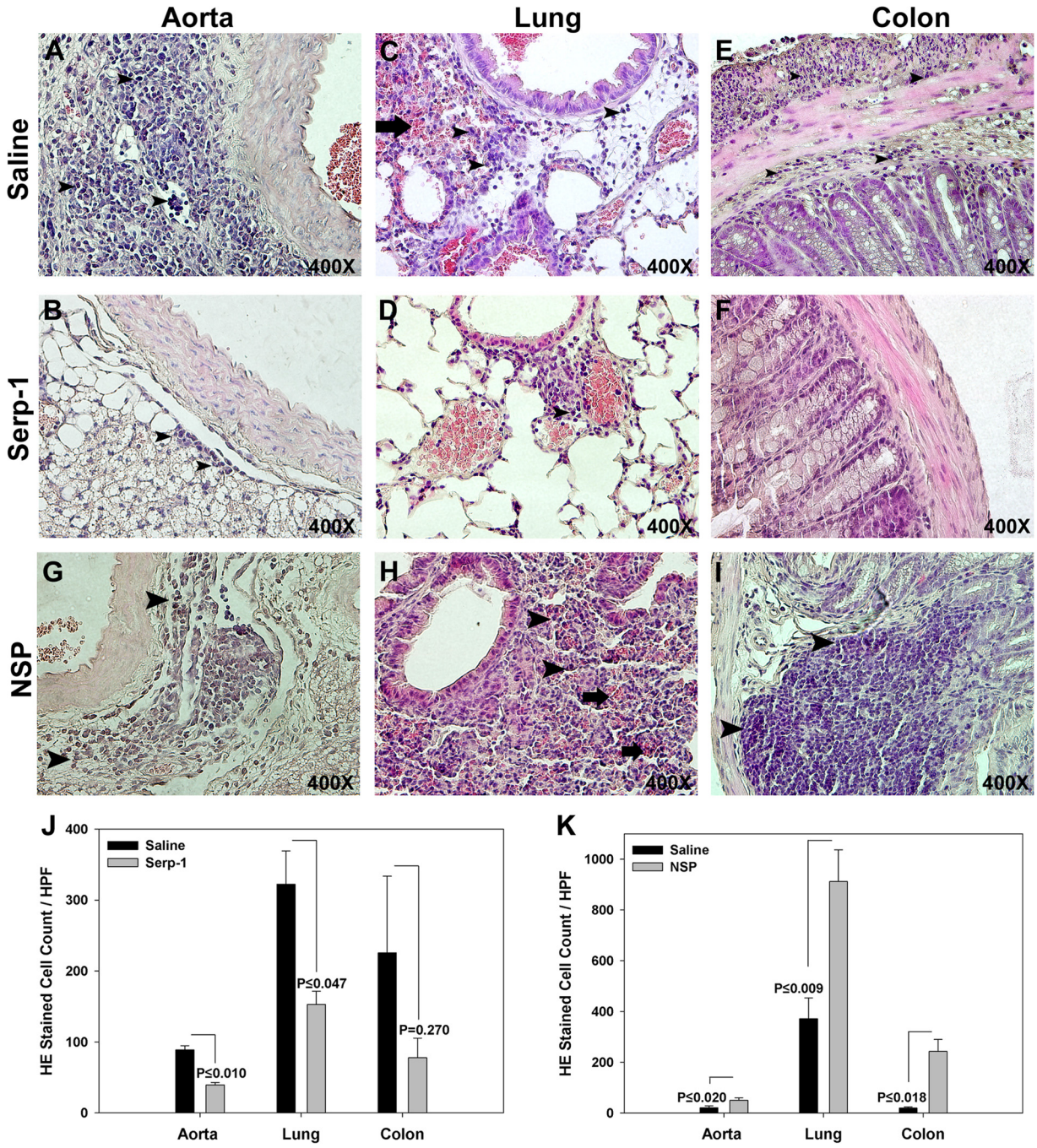

FIG 3 Large inflammatory cell infiltrates were found in the aortic adventitia (A) and lung (C) in saline control-treated MHV68-infected IFN-γR$^{-/-}$ mice at 10 days' follow-up. Serp-1 treatment significantly reduced cell counts in aortic sections (A, B, and J) ($P \leq 0.01$; $n = 14$). Inflammatory cells infiltrates accompanied by hemorrhage and alveolar consolidation are seen in lung sections from saline-treated MHV68-infected control mice (C). Infiltrating cells were reduced after Serp-1 treatment (D and J) ($P \leq 0.047$). Serp-1 treatment produced a nonsignificant reduction in inflammatory cells (F and J) ($P = 0.27$) in colon sections compared to saline (E). Inflammatory cell counts were increased in the aortic adventitia (G and K) ($P \leq 0.02$), lung (H and K) ($P \leq 0.009$), and colon (I and K) ($P \leq 0.018$) in NSP-treated MHV68-infected mice compared to saline controls. Bar graphs demonstrate numbers of invading cells per high-power field, three fields counted per section in Serp-1-treated (J) and NSP-treated (K) MHV68-infected mice compared to saline controls ($n = 14$). Arrowheads indicate the mononuclear cell infiltrates. Thick arrows indicate lung hemorrhage. Cell count is indicated as mean per high-power field ± SE for H&E-stained sections. Magnification, ×400.

J, and N) ($P = 0.197$), lung (Fig. 4H) ($P = 0.172$), or colon on immunostained tissue sections (Fig. 4H) ($P = 0.197$, $P = 0.172$, and $P = 0.490$, respectively).

Serp-1 reduced necrosis and inflammation in the ebolavirus mouse model. Analysis of specimens clearly differentiated treated and nontreated mice after ebolavirus infection. Saline control-treated ebolavirus-infected mice demonstrated severe inflammatory cell invasion with associated necrosis in the spleen (Fig. 5A) and liver (Fig. 5C). These inflammatory and necrotic changes were reduced at higher Serp-1 doses, with significantly reduced spleen

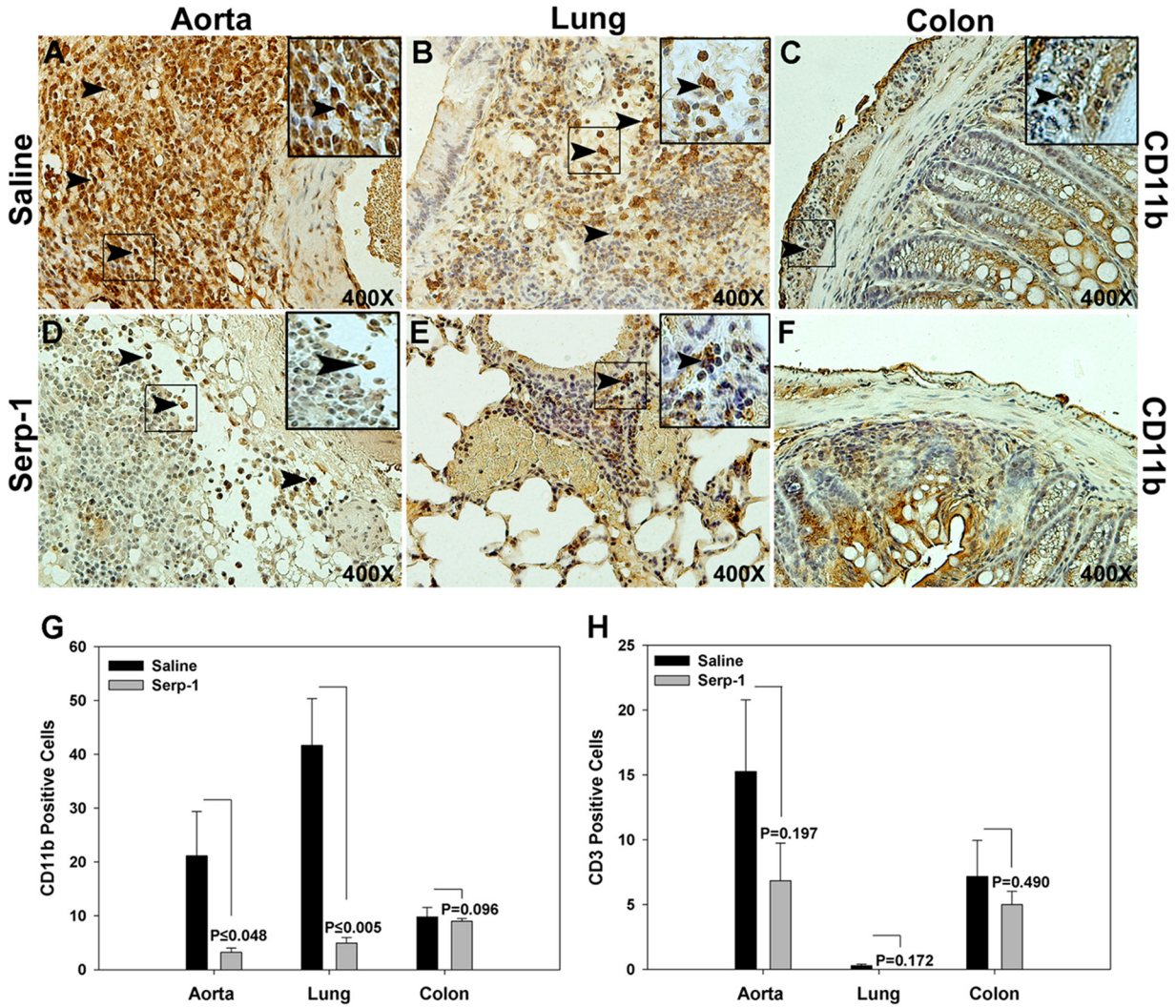

FIG 4 Serp-1 inhibits invasion of $CD11b^+$ but not $CD3^+$ cells into the aorta and lungs in MHV68-infected IFN-$\gamma R^{-/-}$ mice at 10 days' follow-up ($n = 14$). Increased numbers of invading $CD11b^+$ cells were found in the aortic adventitia (A), lung (B), and colon (C) in saline-treated control mice. Serp-1 treatment significantly reduced CD11b-positive cell counts in the aorta (D and G) ($P \leq 0048$) and lung (E and G) ($P \leq 0005$) but not the colon (F and G) ($P = 0.098$) compared to saline controls. $CD3^+$ cells were detected in the aortic adventitia, lung, and colon in saline-treated mice, with smaller numbers in the lung and with nonsignificant decreases in Serp-1-treated mice (H) ($P = 0.197$, 0.172, and 0.49, respectively) ($n = 14$). Positively stained cells are indicated as mean count per HPF ± SE. Arrows indicate $CD11b^+$ cells. Magnification, ×400. Insets represent higher-power (×1,000) magnification.

lymphoid necrosis (Fig. 5B and E) ($P < 0.009$ for 100 μg/kg of Serp-1) and marginal zone hyperplasia (Fig. 5F) ($P < 0.019$ for 50 μg/kg of Serp-1 and $P \leq 0.008$ for 100 μg/kg of Serp-1). There was a trend toward reduced intravascular macrophage counts (Fig. 5G) ($P = 0.06$ for 100 μg/kg of Serp-1). Serp-1 treatment also reduced hepatocyte necrosis at higher doses (Fig. 5D and H) ($P \leq 0.02$).

Neuroserpin and Serp-1 produced opposing effects on immune cell responses in spleen cell isolates. Effects on splenocyte immune cell responses in MHV68-infected mice were assessed in mice treated for 10 days with either Serp-1 or NSP. Splenocytes isolated from one mouse did not provide sufficient counts for flow cytometry analyses; therefore, splenocytes from the same experimental group were pooled and analyzed. We would note that flow analysis is generally considered a qualitative finding and not a quantitative analysis, and we would thus consider these findings to be more qualitative and indicative of trends in cell responses to infection and treatment strategies. Serp-1 selectively increased CD11c cells (macrophages and dendritic cells [DCs]) in the spleen (Fig. 6A) ($P \leq 0.045$) at 10 days. At 5 weeks' follow-up, Serp-1 significantly reduced NK1.1 cells ($P \leq 0.030$) and CD3 CD4 T helper cells ($P \leq 0.046$) but increased CD3 CD8 cytotoxic T cells ($P \leq 0.001$), suggesting a late restoration of sepsis-driven change in immune cell responses (data not shown).

Conversely, NSP significantly reduced a broad spectrum of immune cell responses in the spleen at 10 days (Fig. 6B). Specifically, CD11c (macrophages and dendritic cells; $P \leq 0.010$), CD4 IL-4 (T helper 2 [Th2]; $P \leq 0.023$), CD3 CD8 (Tc cells; $P \leq 0.002$), CCR6 (nonactivated memory T cells and dendritic cells; $P \leq 0.030$), CD19 (B cells; $P \leq 0.008$), CD83 (activated or mature dendritic cells; $P \leq 0.010$) and CD206 (macrophages and dendritic cells; $P \leq 0.035$) cells were reduced, indicating significant systemic effects of NSP on immune responses. NSP treatment could not be

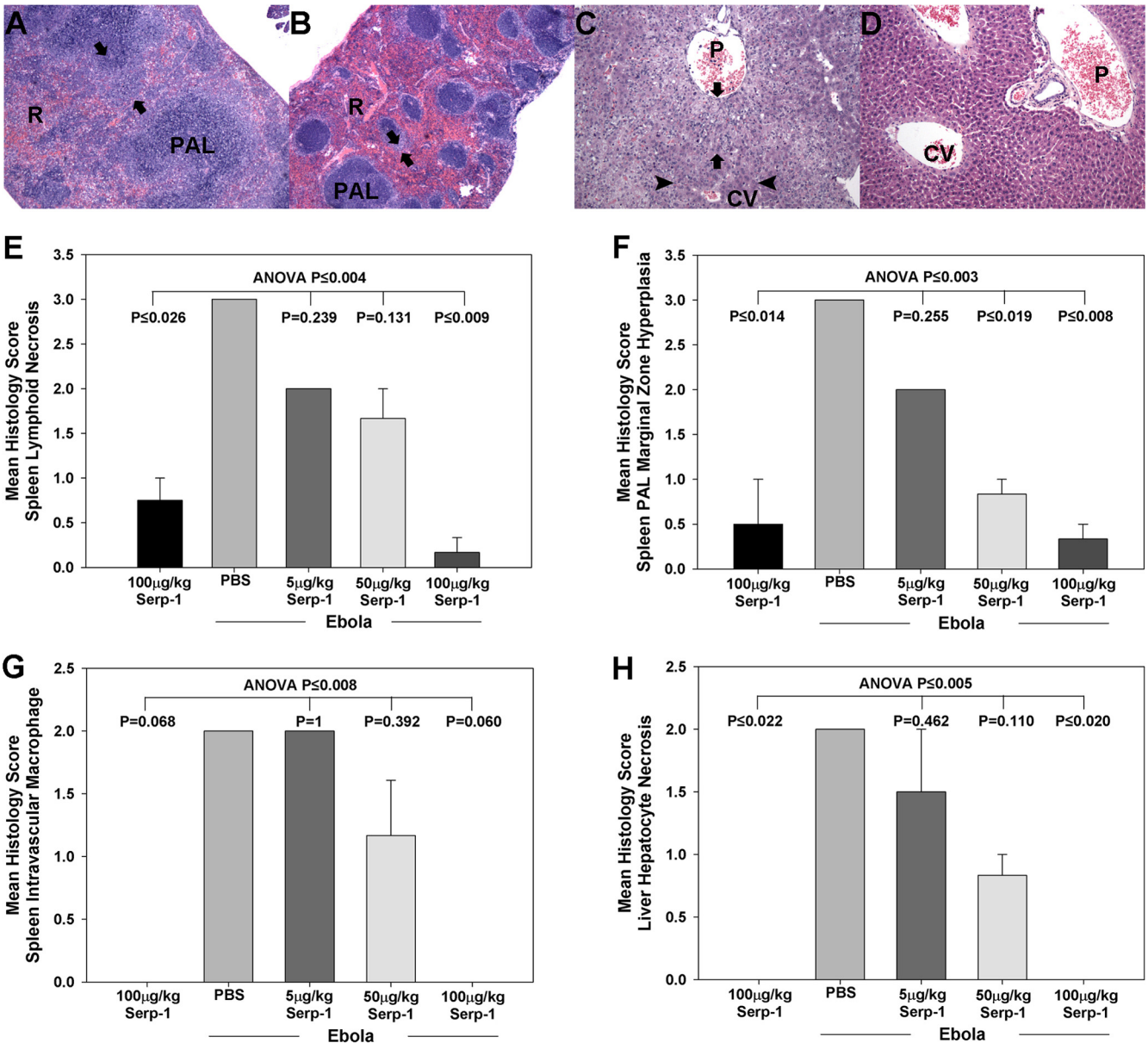

FIG 5 Serp-1 reduced spleen and liver lesions in mouse-adapted Zaire ebolavirus infections in BALB/c mice. H&E-stained sections of spleen (A and B) and liver (C and D) from ebolavirus-infected mice are shown. Control saline-treated sections demonstrate the severe lymphoid hyperplasia of the periarteriolar sheaths (PAL), particularly the marginal zone (arrows) in the spleen (A) that obscures much of the red pulp (R) in infected mice. More normal splenic architecture is seen in the Serp-1 (100 μg/kg/day)-treated mice (B). Moderate to severe necrosis and accompanying inflammation in the periportal and midzonal hepatocytes (arrows) with evidence for severe disruption of the lobular architecture and relative sparing of the central lobular hepatocytes in saline-treated mice can be seen. There is widespread microvesicular lipid degeneration (arrows) and hepatocellular necrosis (arrowheads) disrupting the hepatic cords in control-treated mice (C). Serp-1 markedly reduced evidence for necrosis and tissue damage in hepatic sections (D). P, portal; CV, central vein. Magnification, ×100. Bar graphs demonstrate a clear dose-dependent reduction in spleen lymphoid necrosis (E), marginal zone hyperplasia (F), vascular macrophage invasion (G), and hepatocyte degeneration (H) with Serp-1 treatment at the higher doses. Histology was scored by J. Abbott, blinded to treatment, using a scale of 0 to 5, with increasing severity at higher numbers ($n = 31$); data represent mean scores ± SEs. Magnification, ×100.

assessed at 5 weeks in MHV68-infected mice due to the poor survival. These data suggest that NSP has potential to exacerbate immune dysfunction in sepsis.

Serpin treatments altered serpin and cytokine gene expression. Serp-1 significantly increased aortic gene expression for the regulatory thrombolytic serpins plasminogen activator inhibitor-1 (PAI-1; $P \leq 0.020$) and, unexpectedly, NSP ($P \leq 0.032$; Fig. 7A) in MHV68-infected mouse aortic RNA isolates. The aorta sections of Serp-1-treated mice also had significantly altered expression of inflammatory mediators found in DIC and sepsis, with significant reduction in E selectin ($P \leq 0.048$) (Fig. 7A) and increased IL-10 ($P \leq 0.031$) (Fig. 7A) and addressin ($P \leq 0.002$) (Fig. 7A). Compared to findings for saline-treated mice, NSP decreased gene expression of IL-17 and IL-10 ($P \leq 0.006$ and 0.041, respectively) (Fig. 7A) and increased PAI-2 ($P \leq 0.021$) (Fig. 7A). When comparing Serp-1 and NSP, Serp-1 was found to increase

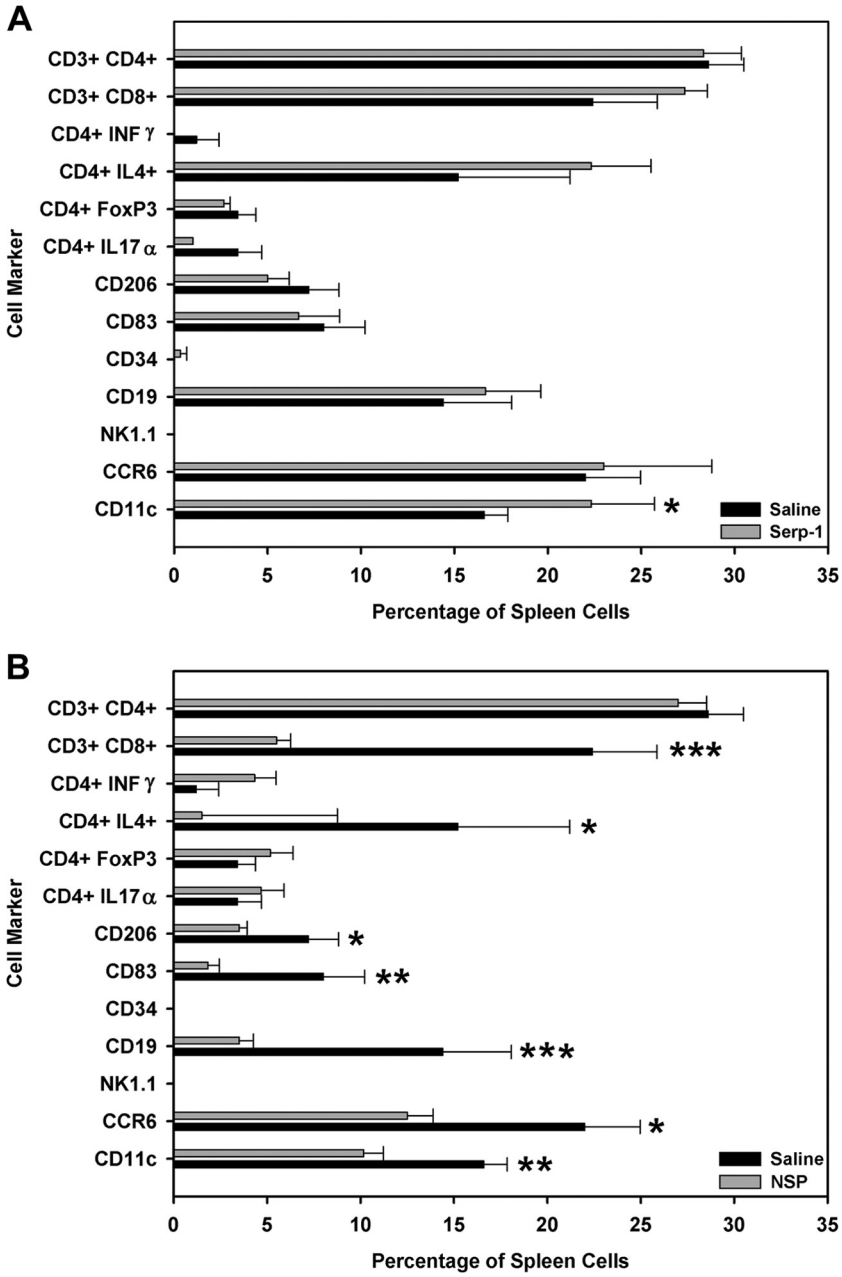

FIG 6 Serp-1 and NSP had opposing effects on splenocyte responses assessed by flow cytometry. Serp-1 significantly increased CD11c counts at 10 days postinfection (A) ($P \leq 0.045$; $n = 14$). Conversely, NSP reduced CD11c (macrophages and DCs; $P \leq 0.010$), CD4 IL-4 (Th2 cells; $P \leq 0.023$), CD3 CD8 (Tc cells; $P \leq 0.002$), CCR6 (nonactivated memory T cells and DCs; $P \leq 0.030$), CD19 (B cells; $P \leq 0.008$), CD83 (mature DCs; $P \leq 0.01$), and CD206 (macrophages and DCs; $P \leq 0.035$) cells at 10 days (B) ($n = 14$). Cell counts are presented as means ± SEs. *, **, and ***, $P \leq 0.05$, $P < 0.01$, and $P < 0.009$, respectively.

IL-10 ($P \leq 0.001$) (Fig. 7A), basic fibroblast growth factor (bFGF) ($P \leq 0.022$) (Fig. 7A), addressin ($P \leq 0.001$) (Fig. 7A), PAI-1 ($P \leq 0.021$) (Fig. 7A), and NSP ($P \leq 0.009$) (Fig. 7A), whereas NSP reduced IL-6 ($P \leq 0.016$) (Fig. 7A) and PAI-2 ($P \leq 0.016$) (Fig. 7A). Serp-1 thus modulated gene expression for serpins that regulate coagulation as well as inflammatory adhesion molecules and cytokines, with overall anti-inflammatory action, while NSP targeted a different set of serpins and cytokines, some with proinflammatory activity. These findings suggest a rebalancing of coagulation and thrombolytic cascades as well as inflammatory and immune responses with Serp-1 treatment.

Serp-1 modified MHV68-induced changes in clotting responses and cytokines. Serp-1 treatment for 10 days significantly increased IL-10 levels in circulating blood ($P < 0.032$) compared to those in the saline-treated controls at 10 days' follow-up after MHV68 infection (Fig. 7B) (34). In contrast, NSP significantly reduced IL-10 levels ($P \leq 0.022$; Fig. 7B) compared to those in saline-treated controls.

MHV68-infected mice had prolonged bleeding times compared to noninfected normal mice at 10 days after infection ($P \leq 0.016$) (Fig. 7C). Serp-1 and NSP treatment reduced bleeding times compared to those obtained with saline treatment ($P \leq 0.046$ and $P \leq$

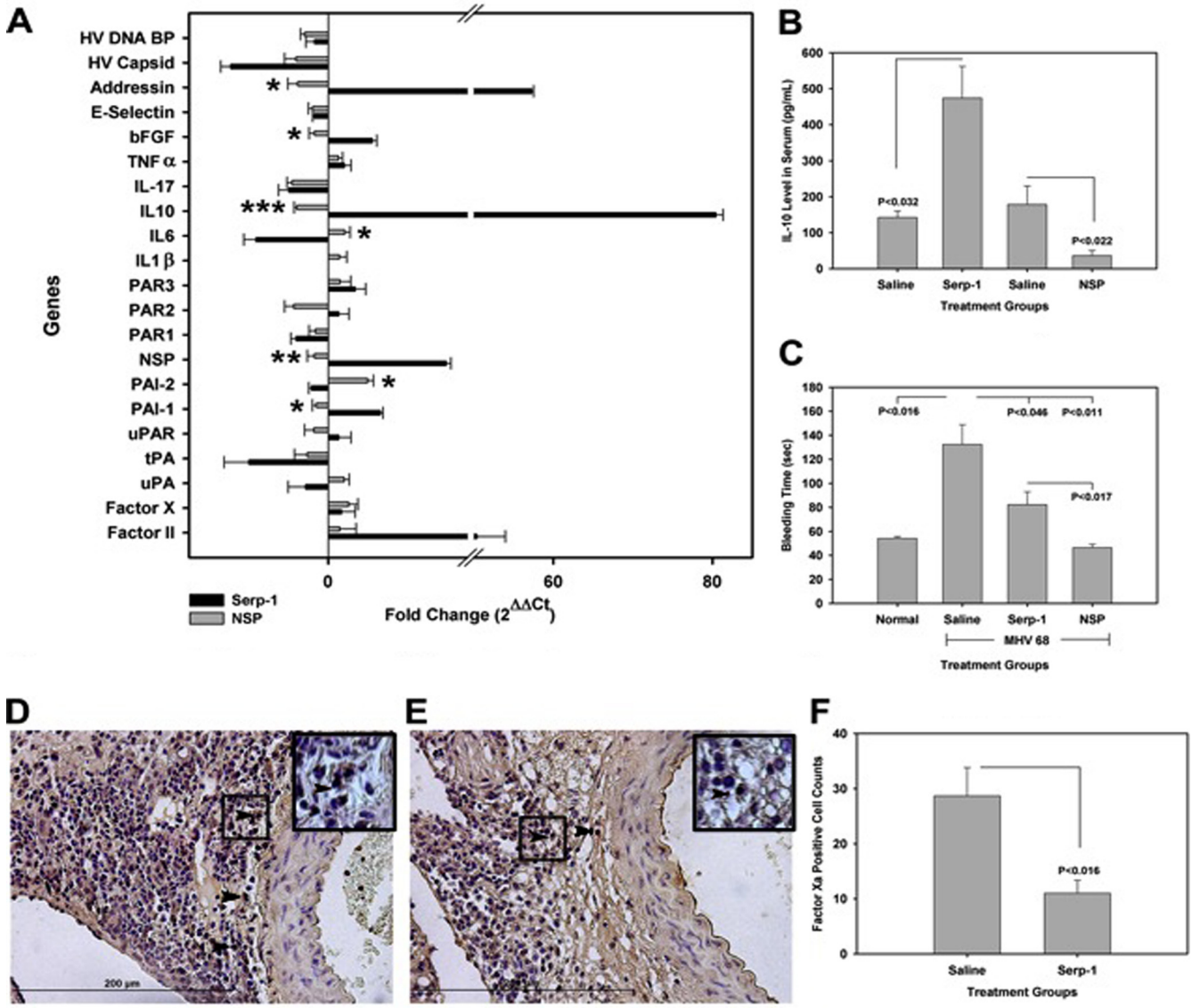

FIG 7 Serp-1 and NSP yielded opposing changes on coagulation and inflammatory pathway gene expression and activity in MHV68-infected mouse aortas at 10 days ($n = 14$). Serp-1 increased gene expression for IL-10 ($P \leq 0.001$), bFGF ($P \leq 0.022$), addressin ($P \leq 0.001$), PAI-1 ($P \leq 0.021$), and NSP ($P \leq 0.009$) and decreased IL-6 ($P \leq 0.016$) and PAI-2 (A) ($P \leq 0.016$), compared to NSP. On immunostained sections, Serp-1 (B) increased IL-10 levels (ELISA) in plasma samples from MHV68-infected mice ($P \leq 0.032$), while NSP reduced IL-10 levels (F) ($P \leq 0.022$). Bleeding time was increased in MHV68-infected mice compared to noninfected mice (C) ($P \leq 0.016$, $n = 14$). Serp-1 and NSP both decreased bleeding time compared to that in MHV68-infected saline controls ($P \leq 0.046$ and $P \leq 0.011$, respectively; $n = 21$). Serp-1 increased bleeding time compared to NSP ($P \leq 0.017$). Serp-1 reduced fXa staining in aortic sections compared to control MHV68-infected mice (E and F) at 10 days compared to saline controls (D and F) ($P \leq 0.016$; $n = 6$). All values are provided as means ± SEs; arrows indicate fXa staining. Magnification, ×400. Insets represent higher-power (×1,000) magnification. *, **, and ***, $P \leq 0.05$, $P < 0.01$, and $P < 0.009$, respectively.

0.011, respectively) (Fig. 7C), as predicted based upon reduced lung hemorrhage. NSP reduced bleeding time more profoundly than did Serp-1 ($P \leq 0.017$) (Fig. 7C). Serp-1 treatment significantly reduced fXa-positive cells in immunostained aortic sections ($P \leq 0.016$) (Fig. 7D, E, and F) from MHV68-infected mice at 10 days.

Thus, Serp-1 treatment for 10 days in MHV68-infected mice was capable of significantly modifying both coagulation responses, reducing bleeding, and anti-inflammatory responses, with increased IL-10. The associated reduction in fXa and increases in gene expression for anti-thrombolytic serpins together with increased IL-10 are associated with a preserved immune cell response, unlike NSP, suggesting that myxomaviral Serp-1 can restore balance to the coagulation cascade and increase anti-inflammatory cytokine responses without significantly suppressing overall immune cell activation.

DISCUSSION

We have examined the effect of treatment with a potent myxomavirus-derived anti-inflammatory purified serpin protein, Serp-1, in an MHV68 model of lethal viral sepsis. Serp-1 improved survival while altering virus load, coagulation, hemorrhage, and inflammatory responses (26, 27). In contrast, a mammalian serpin, neuroserpin, that targets only the thrombolytic serine proteases and not the thrombotic proteases, was ineffective. A second lethal

infection, with mouse-adapted Zaire ebolavirus (4, 28, 29), was also assessed, and in this mouse model, Serp-1 treatment again reduced viral load necrosis and inflammation and improved survival.

Serp-1 improved survival when given starting on the day of infection and remained effective when given starting at 7 days after MHV infection but not when given 21 days after initial infection, suggesting benefit both after incidental exposure and as a prophylaxis for early infections. The fact that Serp-1 improved survival in infections with two unrelated viruses, a herpesvirus and a filovirus, suggests potential for broad applicability in viral sepsis. MHV68 infection is lethal in IFN-γR-deficient mice, which have increased susceptibility to virus infection and in which host immune response is unable to clear the infection. The mouse-adapted Zaire ebolavirus strain is, however, lethal in wild-type BALB/c mice, indicating that the antiviral efficacy displayed by Serp-1 for MHV68 is not limited to IFN-γ receptor-deficient mice or to either DNA or RNA virus infections. In order to examine the mechanism of action of Serp-1, we have focused on the MHV68 infection model.

MHV68 infections in IFN-γR-deficient mice and mouse-adapted Zaire ebolavirus in wild-type BALB/c mice provide models for lethal infections with two separate viral families, representing both DNA and RNA viruses. These differing infections were studied to determine the range of potential efficacy of viral immunomodulating serpin treatments. MHV-68 is widely used as a mouse model for Epstein Barr virus (EBV) and human herpesvirus 8 infections (27–29, 35) and is a well-characterized rodent model for studying gammaherpesviruses. MHV68 infection in IFN-γR-deficient mice provides an extension of this model, with a marked inflammatory cell response and hemorrhage providing a viral sepsis model.

The mouse ebolavirus model is used as an initial model system for assessing the response of ebolavirus to serpin treatment; however, the mouse ebolavirus model is generally considered a model that only partially reproduces ebolavirus infection seen in humans and nonhuman primates (NHPs). Mouse-adapted ebolavirus infections are lethal but are reported not to reproduce the coagulopathy that is observed in humans and NHPs. Thus, future experiments are planned in collaboration with researchers and facilities capable of examining the efficacy of these serpins as therapeutics in the more aggressive level 4 animal models that include the coagulopathy syndrome. We would nevertheless reemphasize that this initial observation using the mouse ebolavirus model provides initial supportive evidence for efficacy in treating a range of differing lethal viral infections that occur both in a knockout model (IFN-γR$^{-/-}$) and in wild-type (BALB/c) mouse models.

Serp-1 targets both thrombotic (fX and fII) and thrombolytic (tPA, uPA, and plasmin) proteases (12–15, 18) and was capable of reducing tissue inflammation and hemorrhage in MHV68-infected mice, whereas mammalian NSP, which targets only thrombolytic cascade proteases (tPA and uPA) (21, 23), was ineffective. This suggests that Serp-1 alters viral sepsis and macrophage invasion through inhibition of fX and/or fII or via combined effects on both thrombotic and thrombolytic (tPA and uPA) pathways. Among MHV68-infected mice, the majority that died had lung consolidation and hemorrhage. Although lung hemorrhage is not seen frequently in this mouse model, alterations in coagulation pathway proteases are known to locally modify innate immunity in affected tissues without overt hemorrhage or fibrin deposition. The mechanism for reduction in pulmonary hemorrhage with Serp-1 treatment in MHV68-infected mice logically may be directly related to inhibition of tPA and uPA. The reduced bleeding time produced by Serp-1 may be the result of inhibition of fX and fII by Serp-1, which may reduce excess coagulation and consumption of clotting factors (consumptive coagulopathy), in septic states. Serp-1 treatment may also result in a combined regulation of both clot-forming and clot lysis pathways (2–10). Thus, Serp-1 may reestablish balance in coagulation pathways in lethal hemorrhagic viral infections. The partial reversal of the prolonged bleeding time and the associated reduction in detectable fX in the aortas of MHV68-infected mice suggest that Serp-1 targets both thrombotic and thrombolytic pathways. PCR array analysis also detected altered gene expression for proteases and serpins (nonsignificant reductions in tPA and uPA and significant increases in fII, NSP, and PAI-1), which may extend this activity. Prior studies with antithrombin and drugs that inhibited only thrombosis or thrombolysis did not prove consistently beneficial (9, 10, 29). Treatment with fX inhibitors in animal models has also indicated a modest improvement in sepsis (35). Combined targeting of both thrombolytic proteases (tPA and uPA) as well as thrombotic proteases fX and fII may enhance efficacy in treating viral sepsis.

Both cascades activate inflammatory cell responses: tPA and uPA, via activation of matrix metalloproteinases and growth factors (14, 18, 36), and thrombin and fX, via activation of protease-activated receptors (PARs) (2, 3, 7, 8), increasing inflammatory cell invasion and activation. MHV68 traffics into the lung by 10 to 12 days after injection, with acute infection of lung and persistent infection in B lymphocytes, epithelial cells, and macrophages (26, 27). Serp-1 dramatically reduced numbers of cells staining positively for MHV68 in the lungs and GI tract compared to saline treatment ($P \leq 0.004$ and $P \leq 0.015$, respectively) and similarly reduced FFU for ebolavirus in liver and blood samples from infected mice. There was an associated significant reduction in invading CD11b-positive macrophages in MHV68-infected mice but no significant reduction in CD3-positive T cells, indicating reduced acute inflammation. Serp-1 may decrease spread and proliferation of unrelated viruses simply by blockade of macrophage or other inflammatory cell invasion (27), or this serpin may represent a defense mechanism by which one virus protects its territory from invasion by other pathogens, e.g., territorial defenses (37). Changes in the microbiome population are known to alter the species of infectious agents living in a host and have been recently reported to alter systemic host immune responses (37, 38). Effects of unrelated viruses on proliferation of other, differing viruses have also been reported previously (37). Serp-1 mediated inhibition of proliferation of other unrelated viruses may thus represent a natural viral defense against invading viruses, or this serpin may simply target pathways central to generation of a septic state.

Arterial inflammatory cell invasion may also be required for virus spread, as blood vessels transport immune cells to infected sites. The arterial wall also acts as a source for clotting factors. On flow cytometry, Serp-1 did not reduce the majority of early cellular responses in spleens at 10 days postinfection, with the exception of an increase in CD11c-positive macrophages and/or dendritic cells. In contrast, NSP produced an early generalized reduction in immune cell responses, with reductions in CD11c, CCR6, CD83, CD206, CD4$^+$ IL-4$^+$, and CD3$^+$ CD8$^+$ cells in MHV68-infected mice. In aortic samples, Serp-1 significantly re-

duced macrophage and increased IL-10 gene expression in MHV68-infected mice, with potential to reduce local aortic inflammation (38). The increased IL-10 in the sera of MHV68-infected mice with Serp-1 treatment may correlate well with prior studies indicating that IL-10 release suppresses macrophage and T cell activation and may be protective in septic states (31–33). Additionally, IL-10 has been reported to modify both thrombotic and thrombolytic activity in sepsis (31, 39). The increase in aortic addressin (VadCAM) (34) conversely would suggest a trend toward increased macrophage activation or potentially a rebalancing of septic immune responses. Thus, Serp-1 may prevent local inflammatory cell invasion and viral dissemination without inducing systemic immune dysfunction, as evidenced in splenocyte analysis. As an opposing response, NSP suppression of a wide array of immune cells may exacerbate immune paralysis induced during viral sepsis.

We postulate that the evolution of potent viral serpins over millions of years has produced new and highly effective immune modulating agents. Serp-1 represents a new class of antimicrobial agent with potential for treatment in severe viral sepsis and DIC. This activity extends the previously demonstrated anti-inflammatory activity in animal models of vascular disease. Viral serpins have previously demonstrated potential for treatment of other systemic inflammation-based disorders, ranging from atherosclerosis, arteritis, and arthritis to transplant rejection. Severe infectious viral and bacterial infections that cause systemic cytokine storm and coagulopathies (DIC) remain an unmet need associated with high mortality and few, if any, effective treatments. For bacterial infections, antibiotic treatments are effective when given early; however, treatment for viral infections remains limited to selected number, and there is associated greater lethality in severe systemic proinflammatory viral infections. With our work and work by others, we propose that the administration of anti-inflammatory serpins targeting the coagulation and inflammatory response systems has therapeutic potential for treatment of disseminated viral sepsis and dysregulated coagulation and inflammation. Serp-1 protein therapy has already been successfully tested in a phase II clinical trial in patients with unstable angina and coronary stent implant, with minimal side effects (24), indicating potential for safe clinical application for systemic inflammatory disorders. In these coronary atherosclerosis patients, D-dimer levels were reduced, indicating potential efficacy under conditions that feature sepsis and DIC (14). We postulate that Serp-1 treatment improves outcomes and survival in lethal viral infections in mice through a dual rebalancing of both thrombotic and thrombolytic cascades as well as promoting anti-inflammatory cell responses through the upregulation of IL-10.

ACKNOWLEDGMENTS

This work was funded by the F008570 Ethel Smith Endowed Vasculitis Research Chair and an NIH ARRA award, 1RC1HL100202. Work with live ebolavirus was funded by the National Microbiology Laboratory of the Public Health Agency of Canada and Viron Therapeutics, Inc. Viron Therapeutics supplied purified Serp-1 protein for these studies but did not fund any of the research with MHV68 or Zaire ebolavirus described in this article.

REFERENCES

1. **Clark IA.** 2007. The advent of the cytokine storm. Immunol. Cell Biol. **85:**271–273.
2. **Chu AJ.** 2010. Blood coagulation as an intrinsic pathway for proinflammation: a mini review. Inflamm. Allergy Drug Targets **9:**32–44.
3. **Esmon C.** 2005. The interactions between inflammation and coagulation. Br. J. Haematol. **131:**417–430.
4. **Bray M, Geisbert TW.** 2005. Ebola virus: the role of macrophages and dendritic cells in the pathogenesis of Ebola hemorrhagic fever. Int. J. Biochem. Cell Biol. **37:**1560–1566.
5. **Semeraro N, Ammollo CT, Semeraro F, Colucci M.** 2012. Sepsis, thrombosis and organ dysfunction. Thromb. Res. **129:**290–295.
6. **Bastarache JA, Ware LB, Bernard GR.** 2006. The role of the coagulation cascade in the continuum of sepsis and acute lung injury and acute respiratory distress syndrome. Semin. Respir. Crit. Care Med. **27:**365–376.
7. **Turpie AG, Esmon C.** 2011. Venous and arterial thrombosis—pathogenesis and the rationale for anticoagulation. Thromb. Haemost. **105:**586–596.
8. **Esmon CT.** 2008. Crosstalk between inflammation and thrombosis. Maturitas **61:**122–131.
9. **Hoffmann JN.** 2006. Benefit/risk profile of high-dose antithrombin in patients with severe sepsis treated with and without concomitant heparin. Thromb. Haemost. **95:**850–856.
10. **Wagner JA, Langenfeld H, Klett L, Störk S.** 2012. Activated protein C in patients with septic shock: a consecutive case series. Int. J. Clin. Pharm. **34:**23–26.
11. **Geisbert TW, Hensley LE, Jahrling PB, Larsen T, Geisbert JB, Paragas J, Young HA, Fredeking TM, Rote WE, Vlasuk GP.** 2003. Treatment of Ebola virus infection with a recombinant inhibitor of factor VIIa/tissue factor: a study in rhesus monkeys. Lancet **362:**1953–1958.
12. **Lucas AR, McFadden G.** 2004. Secreted immunomodulatory viral proteins as novel biotherapeutics. J. Immunol. **173:**4765–4772.
13. **Nash P, Whitty A, Handwerker J, Macen J, McFadden G.** 1998. Inhibitory specificity of the anti-inflammatory myxoma virus serpin, SERP-1. J. Biol. Chem. **273:**20982–20991.
14. **Chen H, Zheng D, Davids J, Bartee MY, Dai E, Liu L, Petrov L, Macaulay C, Thoburn R, Sobel E, Moyer R, McFadden G, Lucas A.** 2011. Viral serpin therapeutics from concept to clinic. Methods Enzymol. **499:**301–329.
15. **Li X, Schneider H, Peters A, Macaulay C, King E, Sun Y, Liu L, Dai E, Davids JA, McFadden G, Lucas A.** 2008. Heparin alters viral serpin, Serp-1, anti-thrombolytic activity to anti-thrombotic activity. Open Biochem. J. **2:**6–15.
16. **Bot I, von der Thüsen JH, Donners MM, Lucas A, Fekkes ML, de Jager SC, Kuiper J, Daemen MJ, van Berkel TJ, Heeneman S, Biessen EA.** 2003. Serine protease inhibitor Serp-1 strongly impairs atherosclerotic lesion formation and induces a stable plaque phenotype in ApoE−/− mice. Circ. Res. **93:**464–471.
17. **Lucas A, Liu L, Macen J, Nash P, Dai E, Stewart M, Graham K, Etches W, Boshkov L, Nation PN, Humen D, Hobman ML, McFadden G.** 1996. Virus-encoded serine proteinase inhibitor, SERP-1, inhibits atherosclerotic plaque development after balloon angioplasty. Circulation **94:**2890–2900.
18. **Lucas A, Liu L, Dai E, Bot I, Viswanathan K, Munuswamy-Ramunujam G, Davids JA, Bartee MY, Richardson J, Christov A, Wang H, Macaulay C, Poznansky M, Zhong R, Miller L, Biessen E, Richardson M, Sullivan C, Moyer R, Hatton M, Lomas DA, McFadden G.** 2009. The serpin saga; development of a new class of virus derived anti-inflammatory protein immunotherapeutics. Adv. Exp. Med. Biol. **666:**132–156.
19. **Bédard EL, Jiang J, Arp J, Qian H, Wang H, Guan H, Liu L, Parry N, Kim P, Garcia B, Li X, Macaulay C, McFadden G, Lucas A, Zhong R.** 2006. Prevention of chronic renal allograft rejection by SERP-1 protein. Transplantation **81:**908–914.
20. **Dai E, Viswanathan K, Sun YM, Li X, Liu LY, Togonu-Bickersteth B, Richardson J, Macaulay C, Nash P, Turner P, Nazarian SH, Moyer R, McFadden G, Lucas AR.** 2006. Identification of myxomaviral serpin reactive site loop sequences that regulate innate immune responses. J. Biol. Chem. **281:**8041–8050.
21. **Munuswamy-Ramanujam G, Dai E, Liu L, Shnabel M, Sun YM, Bartee M, Lomas DA, Lucas AR.** 2010. Neuroserpin, a thrombolytic serine protease inhibitor (serpin), blocks transplant vasculopathy with associated modification of T-helper cell subsets. Thromb. Haemost. **103:**545–555.
22. **Maksymowych WP, Nation N, Nash P, Macen J, Lucas A, McFadden G, Russell AS.** 1996. Amelioration of antigen induced arthritis in rabbits

treated with a secreted viral serine proteinase inhibitor. J. Rheumatol. **23:**878–882.
23. **Irving JA, Ekeowa UI, Belorgey D, Haq I, Gooptu B, Miranda E, Pérez J, Roussel BD, Ordóñez A, Dalton LE, Thomas SE, Marciniak SJ, Parfrey H, Chilvers ER, Teckman JH, Alam S, Mahadeva R, Rashid ST, Vallier L, Lomas DA.** 2011. The serpinopathies studying serpin polymerization in vivo. Methods Enzymol. **501:**421–466.
24. **Tardif JC, L'Allier PL, Grégoire J, Ibrahim R, McFadden G, Kostuk W, Knudtson M, Labinaz M, Waksman R, Pepine CJ, Macaulay C, Guertin MC, Lucas A.** 2010. A randomized controlled, phase 2 trial of the viral serpin Serp-1 in patients with acute coronary syndromes undergoing percutaneous coronary intervention. Circ. Cardiovasc. Interv. **3:**543–548.
25. **Babu GG, Walker JM, Yellon DM, Hausenloy DJ.** 2011. Peri-procedural myocardial injury during percutaneous coronary intervention: an important target for cardioprotection. Eur. Heart J. **32:**23–31.
26. **Dal Canto AJ, Swanson PE, O'Guin AK, Speck SH, Virgin HW.** 2011. IFN-gamma action in the media of the great elastic arteries, a novel immunoprivileged site. J. Clin. Invest. **107:**R15–R22.
27. **Krug LT, Torres-González E, Qin Q, Sorescu D, Rojas M, Stecenko A, Speck SH, Mora AL.** 2010. Inhibition of NF-kappaB signaling reduces virus load and gammaherpesvirus-induced pulmonary fibrosis. Am. J. Pathol. **177:**608–621.
28. **Feldmann H, Geisbert TW.** 2011. Ebola haemorrhagic fever. Lancet **377:**849–862.
29. **Akahane K, Okamoto K, Kikuchi M, Todoroki H, Higure A, Ohuchida T, Kitahara K, Takeda S, Itoh H, Ohsato K.** 2001. Inhibition of factor Xa suppresses the expression of tissue factor in human monocytes and lipopolysaccharide-induced endotoxemia in rats. Surgery **130:**809–818.
30. **Viswanathan K, Richardson J, Togonu-Bickersteth B, Dai E, Liu L, Vatsya P, Sun YM, Yu J, Munuswamy-Ramanujam G, Baker H, Lucas AR.** 2009. Myxoma viral serpin, Serp-1, inhibits human monocyte adhesion through regulation of actin-binding protein filamin B. J. Leukoc. Biol. **85:**418–426.
31. **Minter RM, Ferry MA, Murday ME, Tannahill CL, Bahjat FR, Oberholzer C, Oberholzer A, LaFace D, Hutchins B, Wen S, Shinoda J, Copeland EM, III, Moldawer LL.** 2001. Adenoviral delivery of human and viral IL-10 in murine sepsis. J. Immunol. **167:**1053–1059.
32. **Oberholzer A, Oberholzer C, Bahjat KS, Ungaro R, Tannahill CL, Murday M, Bahjat FR, Abouhamze Z, Tsai V, LaFace D, Hutchins B, Moldawer LL, Clare-Salzler MJ.** 2002. Increased survival in sepsis by in vivo adenovirus-induced expression of IL-10 in dendritic cells. J. Immunol. **168:**3412–3418.
33. **Soderberg KA, Linehan MM, Ruddle NH, Iwasaki A.** 2004. MAdCAM-1 expressing sacral lymph node in the lymphotoxin-deficient mouse provides a site for immune generation following vaginal herpes simplex virus-2 infection. J. Immunol. **173:**1908–1913.
34. **Hsia TY, Ringewald JM, Stroud RE, Forbus GA, Bradley SM, Chung WK, Spinale FG.** 2011. Determinants of extracellular matrix remodelling are differentially expressed in paediatric and adult dilated cardiomyopathy. Eur. J. Heart Fail. **13:**271–277.
35. **Hu JH, Du L, Chu T, Otsuka G, Dronadula N, Jaffe M, Gill SE, Parks WC, Dichek DA.** 2010. Overexpression of urokinase by plaque macrophages causes histological features of plaque rupture and increases vascular matrix metalloproteinase activity in aged apolipoprotein e-null mice. Circulation **121:**1637–1644.
36. **DaPalma T, Doonan BP, Trager NM, Kasman LM.** 2010. A systematic approach to virus-virus interactions. Virus Res. **149:**1–9.
37. **Hooper LV, Littman DR, Macpherson AJ.** 2012. Interactions between the microbiota and the immune system. Science **336:**1268–1273.
38. **Hams E, Saunders SP, Cummins EP, O'Connor A, Tambuwala MT, Gallagher WM, Byrne A, Campos-Torres A, Moynagh PM, Jobin C, Taylor CT, Fallon PG.** 2011. The hydrolase inhibitor dimethyloxallyl glycine attenuates endotoxic shock via alternative activation of macrophages and IL-10 production by B1 cells. Shock **36:**295–302.
39. **Pajkrt D, van der Poll T, Levi M, Cutler DL, Affrime MB, van den Ende A, ten Cate JW, van Deventer SJ.** 1997. Interleukin-10 inhibits activation of coagulation and fibrinolysis during human endotoxemia. Blood **89:**2701–2705.